

## Supplementary Materials for

### **Structure-guided discovery of a single-domain antibody agonist against human apelin receptor**

Yanbin Ma, Yao Ding, Xianqiang Song, Xiaochuan Ma, Xun Li, Ning Zhang, Yunpeng Song, Yaping Sun, Yuqing Shen, Wenge Zhong, Liaoyuan A. Hu, Yingli Ma, Mei-Yun Zhang\*

\*Corresponding author. Email: meiyunz@amgen.com

Published 15 January 2020, *Sci. Adv.* **6**, eaax7379 (2020)  
DOI: 10.1126/sciadv.aax7379

#### This PDF file includes:

- Fig. S1. Binding and thermo-stabilizing effect of JN241 to APJ and formation of stable APJ-JN241 complex and co-crystals.
- Fig. S2. Simple omit maps of JN241 CDR1, CDR2 and CDR3.
- Fig. S3. Characterization of JN241 epitope and identification of the critical residue E174 in APJ ECL2 for its binding and function.
- Fig. S4. Amino acid sequence alignment of JN241 and its nine mutants.
- Fig. S5. Comparison of the receptor-ligand interactions.
- Table S1. Data collection and structure refinement statistics.
- Table S2. Interaction residues on APJ-JN241 interface according to the cocrystal structure.
- Table S3. EC<sub>50</sub> and IC<sub>50</sub> values of JN241 and its mutants fused to human Fc in APJ cAMP and β-arrestin assays.
- Table S4. Conservation of WT APJ, AT1R, and AT2R residues critical for ligand binding.

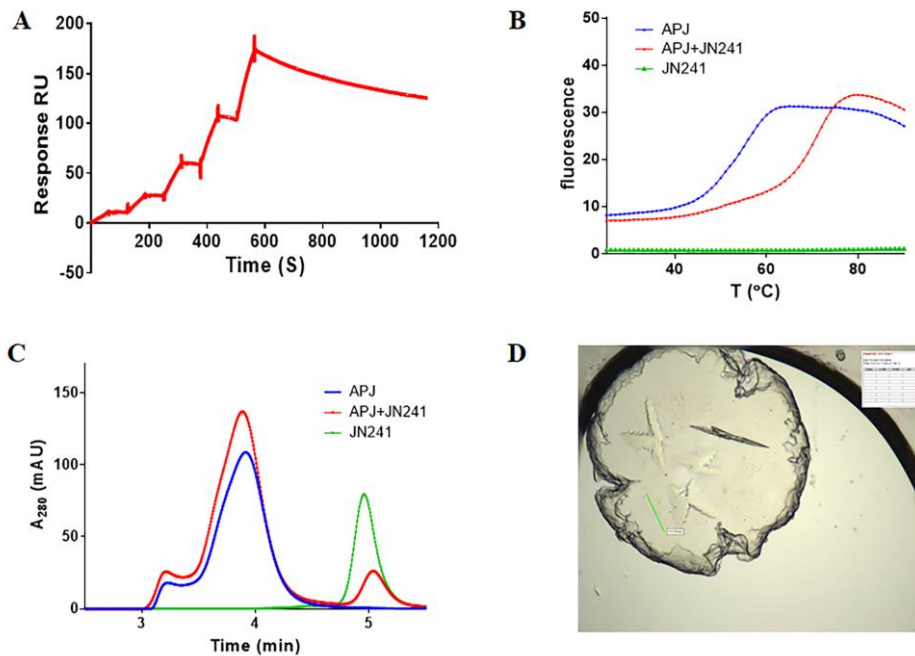


**Fig. S1. Binding and thermo-stabilizing effect of JN241 to APJ and formation of stable APJ-JN241 complex and co-crystals.** Binding (A) and thermo-stabilizing effect (B) of JN241 to APJ and formation of stable APJ-JN241 complex (C) and co-crystals (D). **A.** Potent binding of JN241 to APJ463 nanodiscs by Biacore. APJ463 nanodiscs were immobilized on a SA chip. Soluble JN241 at 10 and 100 nM flew through the surface. Binding kinetics was obtained from curve fitting using Biacore evaluation software. **B.** Thermostability assay of APJ3136 micelles, sdAb JN241, and APJ3136 bound to JN241. **C.** SEC of APJ3136 micelles, sdAb JN241, and APJ3136 complexed with JN241. **D.** Representative co-crystals of APJ3136 in complex with JN241.

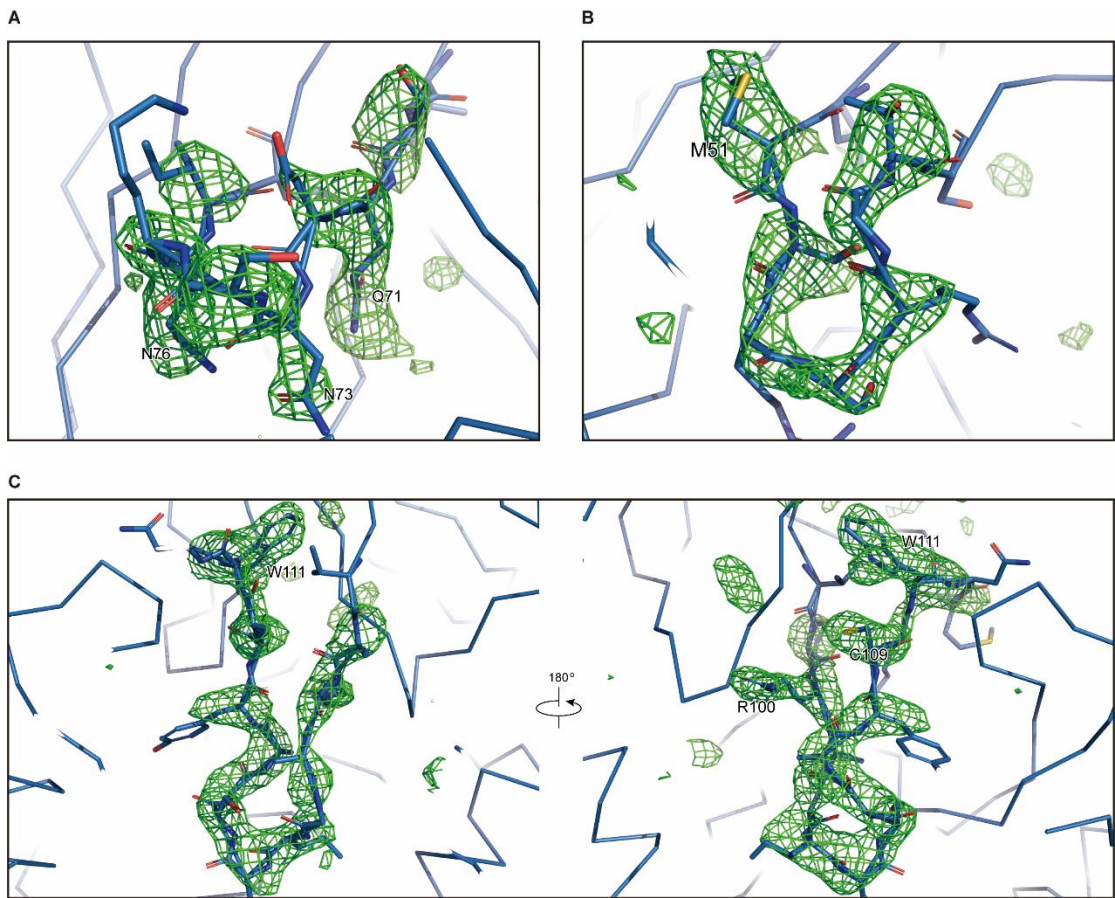


**Fig. S2. Simple omit maps of JN241 CDR1, CDR2 and CDR3.** Simple omit maps (green mesh) of JN241 CDR1 (A), CDR2 (B) and CDR3 (C), showing the  $Fo-Fc$  electron densities contoured at  $3.0\sigma$ . The models of the CDRs are shown in blue sticks.

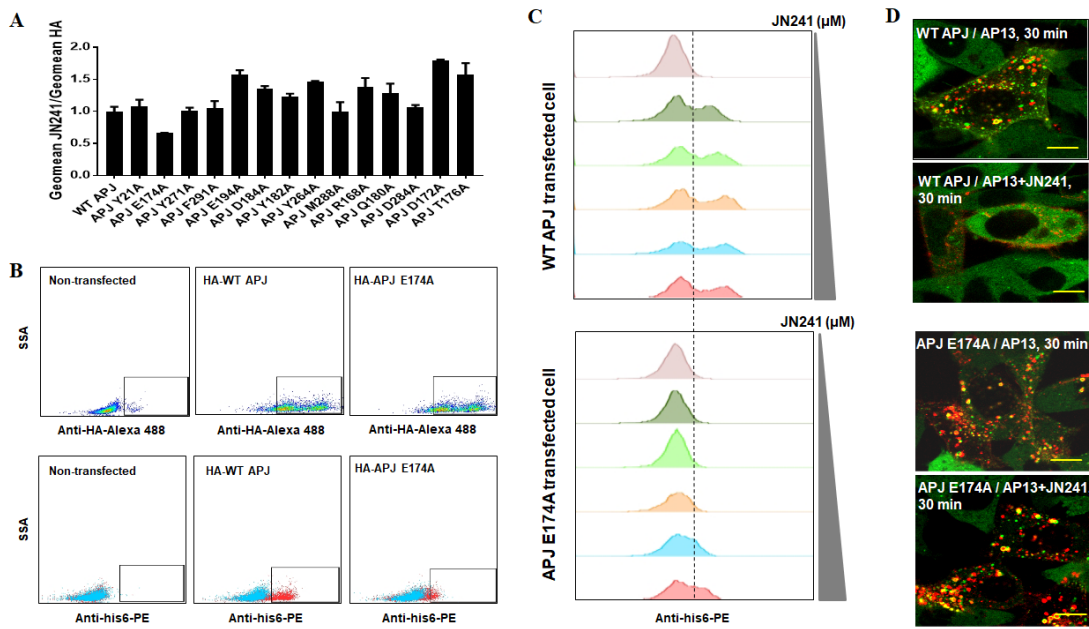


**Fig. S3. Characterization of JN241 epitope and identification of the critical residue E174 in APJ ECL2 for its binding and function.** **A.** Relative binding of soluble sdAb JN241 to 293FT cells transiently expressing HA-tagged WT APJ or APJ site mutants by flow cytometry. Data from representative 14 APJ alanine mutants are shown. **B.** Flow cytometry (dot plots) of parental 293FT cells and HA-tagged WT APJ or APJ E174A mutant transfected 293FT cells stained with either Alexa 488 conjugated to anti-HA antibody or PE conjugated to anti-his6 antibody following 1 $\mu$ M JN241 incubation. blue: No staining control; red: 1 $\mu$ M JN241 stained. **C.** Histogram of flow cytometry with WT APJ or APJ E174A mutant transfected 293FT cells stained with 3-fold serially diluted JN241 with a start concentration of 1  $\mu$ M followed by PE conjugated to anti-his6 antibody. **D.** Confocal microscopy analysis of WT APJ and APJ E174A mutant receptor internalization in response to 100 nM Apelin13 in the presence or absence of 1  $\mu$ M JN241. The re-distribution of APJ (red) and  $\beta$ -arrestin 2 (green) was captured by confocal microscopy in unstimulated status or after the induction with ligand in the presence or absence of JN241 for 30 min. Yellow bar represents 10  $\mu$ m length. AP13: Apelin 13. Arrb2-GFP:  $\beta$ -arrestin 2 fused to GFP.

	FR1	CDR1	FR2	CDR2
JN241	QVQLVESGGSVQSGGSLTLSCAAS	<b>GSTYSSHCMGWF</b> RQAPGKERE <span style="color:red">GVALMTRSRGT</span> SYADSVKGRTFIS		
JN241-1	QVQLVESGGGSVQSGGSLTLSCAAS	<b>GSTYSSHCMGWF</b> RQAPGKERE <span style="color:red">GVALMTRSRGT</span> SYADSVKGRTFIS		
JN241-2	QVQLVESGGGSVQSGGSLTLSCAAS	<b>GSTYSSHCMGWF</b> RQAPGKERE <span style="color:red">GVALMTRSRGT</span> SYADSVKGRTFIS		
JN241-3	QVQLVESGGGSVQSGGSLTLSCAAS	<b>GSTYSSHCMGWF</b> RQAPGKERE <span style="color:red">GVALMTRSRGT</span> SYADSVKGRTFIS		
JN241-4	QVQLVESGGGSVQSGGSLTLSCAAS	<b>GSTYSSHCMGWF</b> RQAPGKERE <span style="color:red">GVALMTRSRGT</span> SYADSVKGRTFIS		
JN241-5	QVQLVESGGGSVQSGGSLTLSCAAS	<b>GSTYSSHCMGWF</b> RQAPGKERE <span style="color:red">GVALMTRSRGT</span> SYADSVKGRTFIS		
JN241-6	QVQLVESGGGSVQSGGSLTLSCAAS	<b>GSTYSSHCMGWF</b> RQAPGKERE <span style="color:red">GVALMTRSRGT</span> SYADSVKGRTFIS		
JN241-7	QVQLVESGGGSVQSGGSLTLSCAAS	<b>GSTYSSHCMGWF</b> RQAPGKERE <span style="color:red">GVALMTRSRGT</span> SYADSVKGRTFIS		
JN241-8	QVQLVESGGGSVQSGGSLTLSCAAS	<b>GSTYSSHCMGWF</b> RQAPGKERE <span style="color:red">GVALMTRSRGT</span> SYADSVKGRTFIS		
JN241-9	QVQLVESGGGSVQSGGSLTLSCAAS	<b>GSTYSSHCMGWF</b> RQAPGKERE <span style="color:red">GVALMTRSRGT</span> SYADSVKGRTFIS		
	FR3	CDR3	FR4	
JN241	QDNTKNILYLQMNSLKPEDTAMYYC	<b>AAVPRAGIE-SGAYCKWNMKD</b> SGSWGQGTLVTVSS		
JN241-1	QDNTKNILYLQMNSLKPEDTAMYYC	<b>AAVPRAGIF-SGAYCKWNMKD</b> SGSWGQGTLVTVSS		
JN241-2	QDNTKNILYLQMNSLKPEDTAMYYC	<b>AAVPRAGIW-SGAYCKWNMKD</b> SGSWGQGTLVTVSS		
JN241-3	QDNTKNILYLQMNSLKPEDTAMYYC	<b>AAVPRAGIY-SGAYCKWNMKD</b> SGSWGQGTLVTVSS		
JN241-4	QDNTKNILYLQMNSLKPEDTAMYYC	<b>AAVPRAGIE-BGAYCKWNMKD</b> SGSWGQGTLVTVSS		
JN241-5	QDNTKNILYLQMNSLKPEDTAMYYC	<b>AAVPRAGIE-WGAYCKWNMKD</b> SGSWGQGTLVTVSS		
JN241-6	QDNTKNILYLQMNSLKPEDTAMYYC	<b>AAVPRAGIE-YGAYCKWNMKD</b> SGSWGQGTLVTVSS		
JN241-7	QDNTKNILYLQMNSLKPEDTAMYYC	<b>AAVPRAGIEFSGAYCKWNMKD</b> SGSWGQGTLVTVSS		
JN241-8	QDNTKNILYLQMNSLKPEDTAMYYC	<b>AAVPRAGIEFWSGAYCKWNMKD</b> SGSWGQGTLVTVSS		
JN241-9	QDNTKNILYLQMNSLKPEDTAMYYC	<b>AAVPRAGIEYESGAYCKWNMKD</b> SGSWGQGTLVTVSS		

**Fig. S4. Amino acid sequence alignment of JN241 and its nine mutants.** Mutations are in red and highlighted in the rectangular frame.

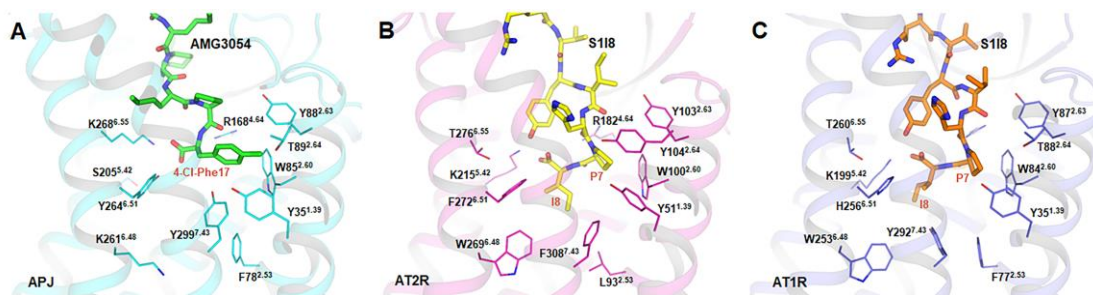


**Fig. S5. Comparison of the receptor-ligand interactions.** **A.** APJ-AMG3054 (PDB ID: 5VBL); **B.** AT2R-S1I8 (PDB ID: 5XJM); **C.** AT1R-S1I8 (PDB ID: 6DO1). APJ (in cyan), AT2R (in magenta) and AT1R (in blue) are shown as cartoons. The ligands AMG3054 (in green), S1I8 (in yellow) and S1I8 (in orange) are shown as sticks. APJ, AT2R and AT1R residues at the bottom of the orthosteric sites are shown as lines.

**Table S1. Data collection and structure refinement statistics.**

APJ-JN241	
<b>Data collection</b>	
Space group	P2 <sub>1</sub> 2 <sub>1</sub> 2 <sub>1</sub>
Cell dimensions	
<i>a, b, c</i> (Å)	44.78, 48.39, 350.10
$\alpha, \beta, \gamma$ (°)	90.00, 90.00, 90.00
Resolution (Å)	50-3.2(3.28-3.20)*
$R_{\text{merge}}$ (%)	19.4(39.6)
$I / \sigma I$	4.38(1.86)
Completeness (%)	92.5(62.1)
Redundancy	3.2(1.8)
<b>Refinement</b>	
Resolution (Å)	46.6-3.2
No. reflections	12359
$R_{\text{work}} / R_{\text{free}}$ (%)	25.6/30.1
No. atoms	
Protein	3742
Ligand/ion	1
<i>B</i> -factors	
Protein	97.40
Ligand/ion	82.86
R.m.s. deviations	
Bond lengths (Å)	0.014
Bond angles (°)	1.403
Ramachandran plot statistics (%)	
Favored	88.14
Allowed	11.86
Disallowed	0

\*Values in parentheses are for highest-resolution shell.

**Table S2. Interaction residues on APJ-JN241 interface according to the cocrystal structure.**

Interaction residue on APJ	Location of the residue on APJ	Corresponding interaction residue on JN241	Location of the residue on JN241	Nature of the interaction
GLU20	N-terminus	SER70	FR3	Hydrogen Bond
		GLN71 (backbone)	FR3	Hydrogen Bond
		CYS33	CDR1	Hydrophobic
TYR21	N-terminus	CYS33 (backbone)	CDR1	Hydrogen Bond
		MET34 (backbone)	FR2	Hydrogen Bond
		MET51	CDR2	Hydrophobic
ASP92	TM2	GLN71	FR3	Hydrogen Bond
		ARG53	CDR2	Electrostatic
		TYR108	CDR3	Hydrophobic
ARG168	TM4	GLU104	CDR3	Electrostatic
		GLU104 (backbone)	CDR3	Hydrogen Bond
LEU173	ECL2	MET113	CDR3	Hydrophobic
		THR52	CDR2	Hydrogen Bond
		SER54	CDR2	Hydrogen Bond
GLU174	ECL2	CYS109 (backbone)	CDR3	Hydrogen Bond
		ASN175 (backbone)	CDR2	Hydrogen Bond
TYR182 (backbone)	ECL2	ARG55	CDR2	Hydrogen Bond
MET183 (backbone)	ECL2	SER105	CDR3	Hydrogen Bond
ASP184	ECL2	SER105	CDR3	Hydrogen Bond
VAL191	ECL2	LYS110	CDR3	Hydrogen Bond; Electrostatic
SER192	ECL2	PRO99	CDR3	Hydrophobic
GLU194	TM5	GLN1 (backbone)	FR1	Hydrogen Bond
GLU198	TM5	LYS110	CDR3	Electrostatic
TYR264	TM6	GLY102 (backbone)	CDR3	Hydrogen Bond
TYR271	TM6	GLU104	CDR3	Hydrogen Bond
		SER30 (backbone)	CDR1	Hydrogen Bond
SER275	TM6	ILE103	CDR3	Hydrophobic
CYS281	TM7	SER30	CDR1	Hydrogen Bond
ASP284	TM7	TYR29	CDR1	Pi-Sulfur
MET288	TM7	ALA107	CDR3	Hydrophobic
PHE291	TM7	ILE103	CDR3	Hydrophobic
		ILE103-GLU104 (backbone)	CDR3	Hydrophobic

**Table S3. EC<sub>50</sub> and IC<sub>50</sub> values of JN241 and its mutants fused to human Fc in APJ cAMP and β-arrestin assays.**

JN241 mutant fusion to human Fc	Mutations or insertions at position E104 and S105	EC <sub>50</sub> (M) in cAMP assay	IC <sub>50</sub> (M) in cAMP assay	EC <sub>50</sub> (M) in β-arrestin assay	IC <sub>50</sub> (M) in β-arrestin assay
Apelin13	/	6.72E-10	/	5.41E-10	
JN241-1	<b>FS</b>	/	2.12E-08		
JN241-2	<b>WS</b>	/	1.74E-08		
JN241-3	<b>YS</b>	/	2.05E-08		
JN241-4	<b>EF</b>	/	5.15E-08		
JN241-5	<b>EW</b>	/	4.79E-08		
JN241-6	<b>EY</b>	/	4.75E-08		
JN241-7	E[F]S	1.51E-07	1.66E-08*	3.12E-08	/
JN241-8	E[W]S	/	3.39E-08	/	> 1.00E-7
JN241-9	E[Y]S	3.58E-08	/	4.70E-08	/
JN241-Fc	/	/	3.08E-08	/	> 1.00E-7

Mutations or insertions are in bold. [ ]: Insertions. “/”: Non-functional. \*: Partial agonist. Blank: Not tested.

**Table S4. Conservation of WT APJ, AT1R, and AT2R residues critical for ligand binding.** Identical amino acids are highlighted in bold.

Location	1.39	2.53	2.60	2.63	2.64	4.64	5.42	6.48	6.51	6.55	7.43
WT APJ	<b>Y35</b>	<b>F78</b>	<b>W85</b>	<b>Y88</b>	<b>T89</b>	<b>R168</b>	S205	<b>W261</b>	Y264	K268	<b>Y299</b>
WT AT1R	<b>Y35</b>	<b>F77</b>	<b>W84</b>	<b>Y87</b>	<b>T88</b>	<b>R167</b>	<b>K199</b>	<b>W253</b>	H256	<b>T260</b>	<b>Y292</b>
WT AT2R	<b>Y51</b>	L93	<b>W100</b>	<b>Y103</b>	Y104	<b>R182</b>	<b>K215</b>	<b>W269</b>	F272	<b>T276</b>	F308